

Prediction of Transient Transfer Functions at Cable-Transformer Interfaces

Joe Y. Zhou, *Member, IEEE* and Steven A. Boggs, *Fellow, IEEE*

Abstract - Lightning and switching surges are the most common causes of electrical failures in distribution transformers. Fast rising transients that reach the transformer can cause large turn-to-turn voltages at the line end of the windings and resonances, which result in large voltages to ground elsewhere in the windings, many of which may exceed the winding insulation strength. In a previous paper [1], empirical data were presented which indicate that the type of cable employed between the source of the transient and the transformer has an impact on the electrical stress imposed on the transformer. The present contribution takes a more analytical approach to this work, and establishes the factors which play a role in this difference, the most important of which appears to be the loss of the cable dielectric.

Index Terms - Cable insulation, circuit breakers, pulse generation, pulse measurements, power cable, power transformers, transient propagation, transformer windings.

INTRODUCTION

Measurements were carried out of the effect of various types of distribution cables on the transients incident on distribution transformers. An impulse generator and spark gap were used to produce relatively fast transients at the input to the cable (Figure 1). The transformer tested was a 150 kVA, three-phase unit rated 13,200 volts delta, with 208 Y/120 volts secondary. Although the transformer was a 3-phase unit, all tests were on one phase. The inductive load on the secondary side of the transformer was the primary of a 50 kVA single phase transformer, rated 7620/13200Y to 120/240 volts secondary, with the secondary windings open-circuited. Inductance was used because reported field failures have generally been associated with light load conditions when power factor has been extremely low and highly inductive. Experiments on the setups with and without inductance verified that voltage transients were more pronounced with the inductance present.

A Tektronix four channel digital oscilloscope and high voltage probes were used to measure the voltage at the input to the cable and at the interface between the cable and transformer (Figure 2). An MOV arrester was included in the circuit to protect the equipment. In order to simulate this direct stroke, an im-

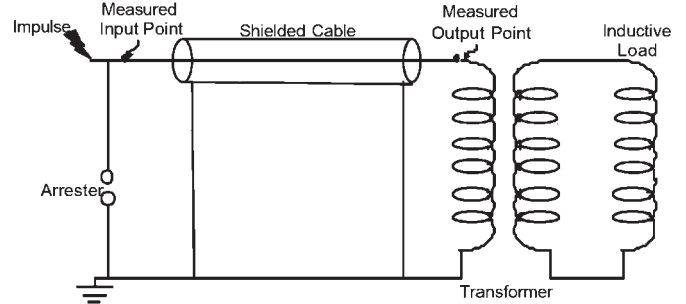


Figure 1. Experimental configuration employed to determine the effect of various distribution cables on the transient which reaches a transformer.

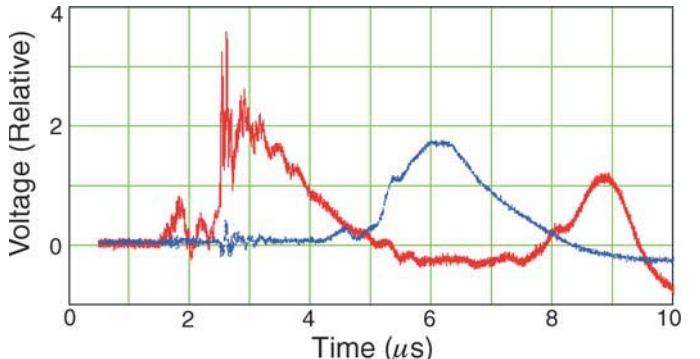


Figure 2. Voltage at the input to the cable (red) and at the interface between the cable and transformer (blue) after propagation through 400 m of EPR 2 cable. The "bump" in the red signal at about 9 μ s is caused by the return of the signal reflected from the transformer to the cable input.

pulse generator was charged to one million volts and discharged into the cables under test, shunted by a set of adjustable sphere gaps. This setup produced effective rise times in the order of 50 to 100 nanoseconds.

The cable construction tested was one that is representative of medium voltage underground residential cable. The authors selected #2AWG, 7 strand, aluminum 15kV, 100% insulated (175 mils), with a full neutral (10, #14AWG bare copper wires), and with an encapsulating overall polyethylene jacket. Three insulation types were tested – TR-XLPE, EPR1, and EPR2. The cable length (Figure 1) was varied from 50 to 800 meters.

DETERMINATION OF TRANSFER FUNCTIONS

A previous paper [1] analyzed the data in the time domain, i.e., the effect of the cable on the risetime (dV/dt) of the surge incident on the transformer as a function of cable length. In the present paper, we take two approaches:

Joe Zhou participated in this work while completing his Ph.D. at the University of Connecticut. He is presently with the Global Research Center of the General Electric Company in Niskayuna, NY 12309 (yzhou@ieee.org).

Steven Boggs is Director of the Electrical Insulation Research Center, Institute of Materials Science, University of Connecticut, 97 N. Eagleville Rd., Storrs, CT 06269-3136 (steven.boggs@ieee.org)

1. We determined the transfer function in the frequency domain between the input and output of the cable by dividing the Fourier components of the output by those of the input.
2. We predict the transfer function from the input to the output based on (i) computing the Fourier components of the input and multiplying them by the frequency dependent attenuation appropriate for the length and type of the cable based on the measured cable attenuation and (ii) assuming that the waveform that appears across the terminals of the cable is that computed in (i) modified by the frequency-dependent division caused by the cable and transformer impedances. Thus if the characteristic impedance of the cable were 35 Ohms, which is typical, and the frequency-dependent impedance of the transformer were $Z_t(f)$, the voltage which appears across the terminals of the transformer would be the voltage at the end of the cable times $(2 Z_t(f))/(35+Z_t(f))$. The factor of two comes in because if you terminate the cable in its characteristic impedance, you get the full voltage across that impedance, not half.

The impedance of the transformer with the inductance across the secondary, as described above, was measured using two impedance analyzers which, together, cover the range from 20 Hz to 1 GHz. Useful data were obtained from 10 kHz to 40 MHz (Figure 3). As will be seen below, the input waveforms did not have useful signal energy above 30 MHz.

The first step in the analysis is to isolate the input signal and condition it so that it starts and ends at the same value, as a Fourier transform assumes a periodic waveform and any step between the beginning and end of the waveform is “interpreted” as a step with large high frequency content. The waveform was forced to zero in its tail by multiplying the measured data by an exponential which went to zero with increased time beyond that point in the waveform. The resulting typical input waveform for the analysis is shown in Figure 4. The data were padded with zeros to create exactly 8192 data which resulted in a frequency resolution of about 100 kHz, i.e., the Fourier coefficients were separated by about 100 kHz in frequency. The magnitude of the Fourier coefficients vs frequency is shown in Figure 5. The noisy nature of the coefficients above 30 MHz indicates a lack of useful signal energy in this frequency range. This was confirmed by truncating the Fourier series at 30 MHz and reconstructing the time domain waveform. The only effect of the truncation was to eliminate high frequency noise from the waveform.

Figure 6 shows an example of data measured at the output of the cable (the interface between the cable and transformer). These data have been prepared as those in Figure 4, by forcing the data to zero beyond a certain time and padding the data with zeros to obtain exactly 8192 data. Data such as those in Figures 4 and 6 were next aligned in time, i.e., the waveforms were shifted until the wavefronts aligned in time. The Fourier trans-

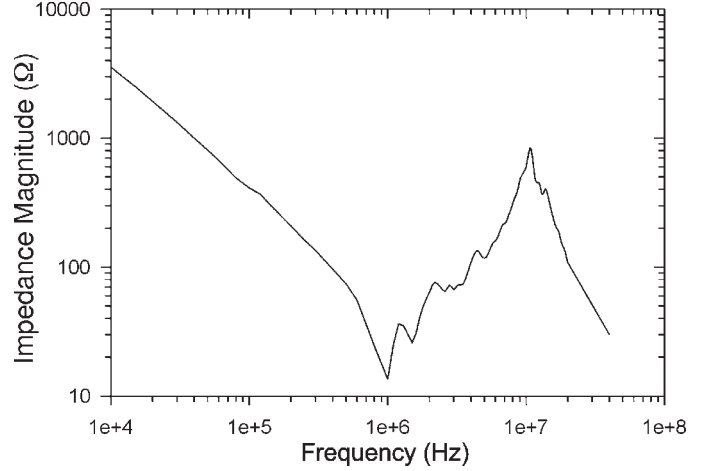


Figure 3. Measured transformer impedance from 10 kHz to 40 MHz. The impedance was measured with the inductance across the secondary, as was employed during the impulse testing. The data from the two impedance analyzers overlap at 1 MHz, where both data are plotted. The difference between the two measurements at 1 MHz is so small as to be invisible in the above plot.

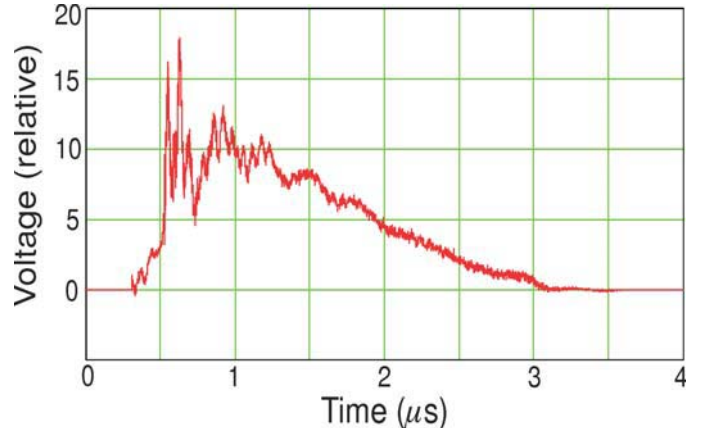


Figure 4. Example of data measured at the cable input as prepared for FFT to determine the Fourier coefficients as a function of frequency. The waveform has been forced to zero beyond about $3.2\mu s$ and padded to exactly 8192 data.

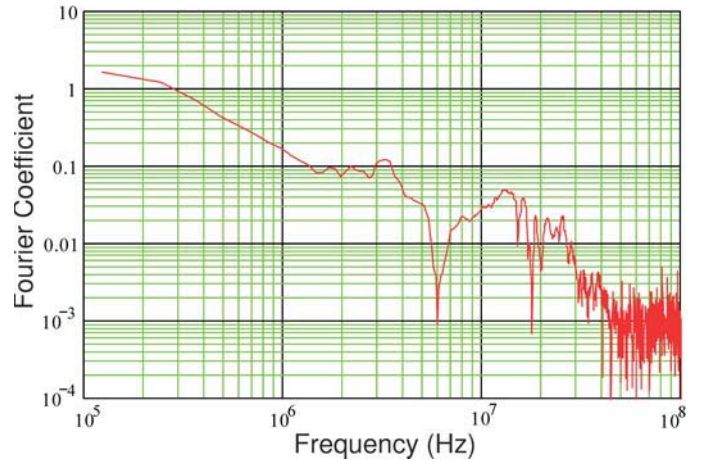


Figure 5. Fourier coefficients vs frequency from the FFT of Figure 4. The frequency resolution is about 100 kHz. The random nature of the Fourier coefficients above 30 MHz indicates that no use signal exists in this frequency range. This was confirmed by truncating the Fourier series at 30 MHz and reconstructing the time domain signal. The only effect was to remove high frequency noise from the signal.

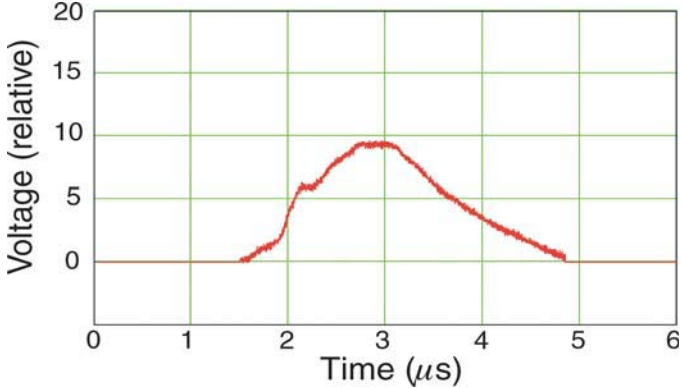


Figure 6. Example of data measured at the cable output (cable-transformer interface) as prepared for FFT. The waveform has been forced to zero beyond about 5 ms and padded with zeros to exactly 8192 data.

form of the input and output data were then computed, along with the ratio thereof to determine the transfer function, a typical example of which for TR-XLPE and EPR2 cable are shown in Figure 7. Clearly the EPR2 cable provides greater attenuation above about 700 kHz than does the TR-XLPE cable, which was new at the time and may have exhibited a greater attenuation than would occur after loss of manufacturing byproducts from the dielectric.

CABLE ATTENUATION

The effect of cable attenuation on transients in power systems has been studied extensively [2-5]. For the present study, the cable attenuation was measured using the same two impedance analyzers as used to measure the transformer impedance. Figure 8 shows a comparison of the measured attenuations for EPR2 cable and the TR-XLPE cable. As expected from Figure 7, the attenuation of the EPR2 cable is appreciably greater than that of the TR-XLPE cable.

COMPUTATION OF TRANSFER FUNCTIONS

The transfer function can be predicted from the measured cable attenuations and the measured transformer impedance based on the circuit of Figure 9. The transfer function is computed in two steps. In Step 1 (Figure 9), the effect of the cable attenuation is computed in the frequency domain based on the measured attenuation thereof. In Step 2, the cable-attenuated signal is applied through the characteristic impedance of the cable to the measured impedance of the transformer. The cable and transformer form a frequency-dependent divider, from which the resulting waveform at the cable-transformer interface can be computed in the frequency domain and transformed back to the time domain. The factor of 2 results from the fact that if the cable were terminated in its characteristic impedance, the division ratio would be unity. Figure 10 shows a typical example of the transfer function computed on this basis (black) in comparison with the transfer function computed from the data measured at the input and output of the cable (red). Agreement is quite good to about 2 MHz but deviates substantially at higher frequencies.

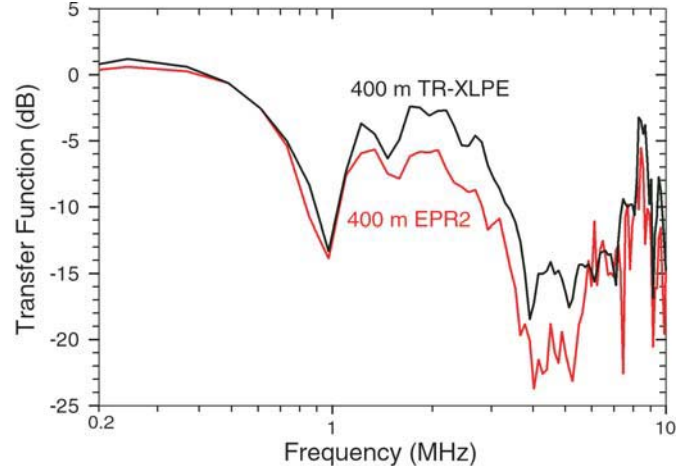


Figure 7. Transfer function from the input of the cable to the interface between the cable and transformer with 400 m of TR-XLPE cable and 400 m of EPR2 cable. The EPR2 cable clearly has appreciably greater attenuation above about 700 kHz. The data beyond about 5 MHz are dominated by noise.

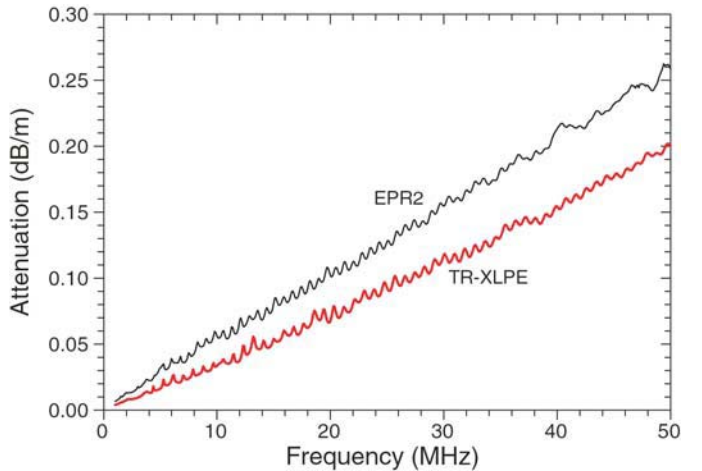
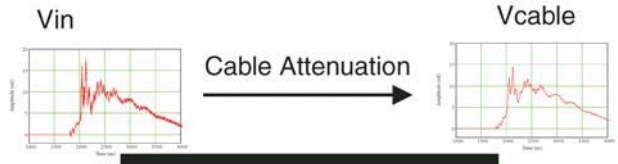


Figure 8. Measured attenuation of EPR2 and TR-XLPE cables.

Step 1: Compute Effect of Cable



Step 2: Compute effect of Cable-Transformer

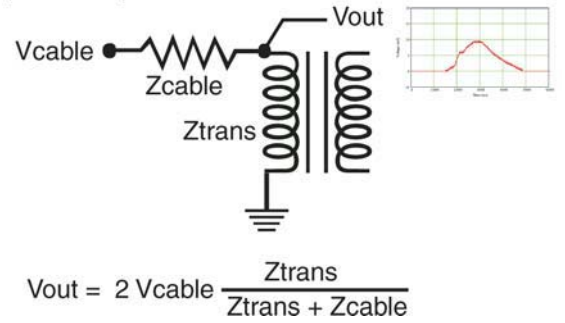


Figure 9. Approach to computation of the transfer function from the measured cable attenuation and the measured transformer impedance.

This suggests that the transformer impedance in this frequency range is much lower than that shown in Figure 3 for frequencies above 2 MHz. The above approach is reasonable if the cable is sufficiently long that it maintains its characteristic impedance over the range of frequencies and times involved in the analysis. A more rigorous approach would be to compute the impedance at the input of the cable as a function of frequency using the measured propagation characteristics of the cable, which were determined during measurement of the cable attenuation. Unfortunately the cable impedance measurement is sufficiently arduous to provide a good measure of the cable attenuation, but not sufficiently accurate to provide reasonable data using this approach to computing the transfer function. When this approach was attempted, the resulting transfer function was extremely noisy. However insofar as the two approaches could be compared in spite of this noise, the resulting transfer function did not differ greatly and the more rigorous approach did not reproduce the large attenuation in the region of 3 to 7 MHz.

EFFECT OF DIFFERENCES BETWEEN CABLES

We can compare the difference between the transfer functions for EPR2 and TR-XLPE cable in Figure 7 with the difference in cable attenuation over 400 m based on Figure 8. These differences are compared in Figure 11, which tends to indicate that the difference in cable attenuation accounts for most of the difference in transfer function. The primary difference among the cables is dielectric loss, and for cable EPR2, this loss is quite significant, as can be seen from the "loss budget" for the EPR2 cable shown in Figure 12. Note that the sum of the loss mechanisms adds quite precisely to the measured cable loss, largely because the loss caused by the interaction of the neutral wires with the ground shield semicon has been computed accurately for the first time. This loss mechanism has never been discussed in the literature but has recently been studied by the authors and their colleagues. Details will be published in the near future.

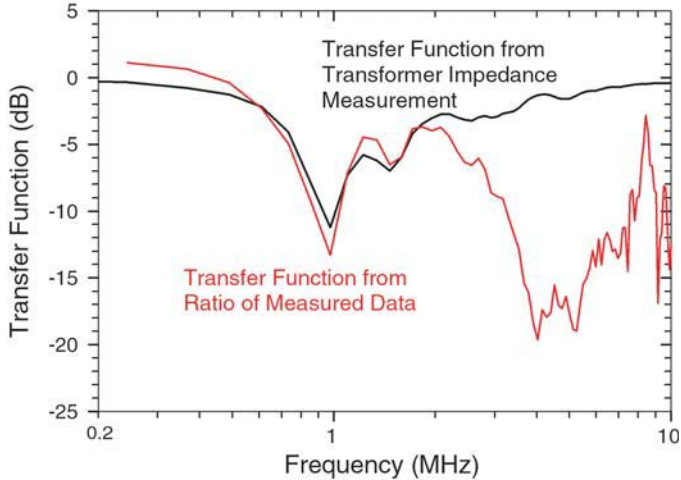


Figure 10. Transfer functions computed from measured data at the two ends of the cable (red) and from the measured cable attenuation and transformer impedance (black).

The contribution of the dielectric loss, as shown in Figure 12, has been computed for a 400 m cable length of EPR2 and plotted in Figure 11. Given that the dielectric loss of polyethylene based dielectrics is generally negligible at high frequencies, the result suggests that the difference in the loss of the dielectric accounts for most of the difference in cable attenuation, as would be expected. The remaining difference is most likely to be dominated by differences in the high frequency impedance characteristics of the ground shield semicon, which change the loss caused by the interaction of the neutral wires with the ground shield semicon.

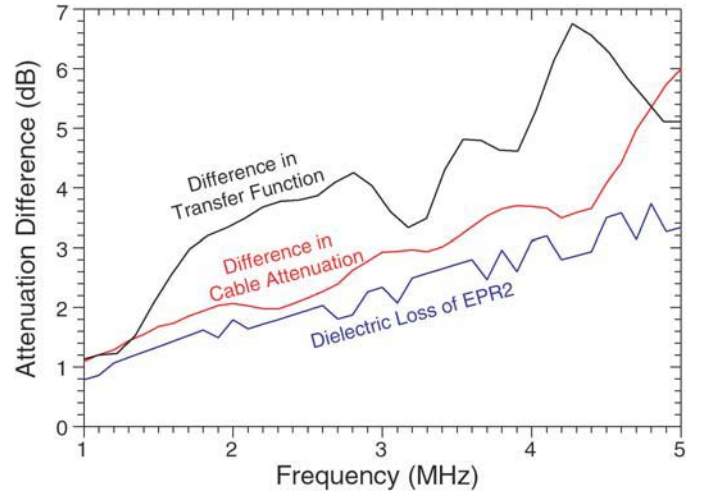


Figure 11. Difference in cable attenuation over 400 m between EPR2 cable and TR-XLPE cable (Figure 8) compared with the difference in transfer function at the cable-transformer interface with 400 m of EPR2 cable vs TR-XLPE cable (Figure 7). The comparison suggests that most of the difference in transfer function results from the difference in cable attenuation, as would be expected.

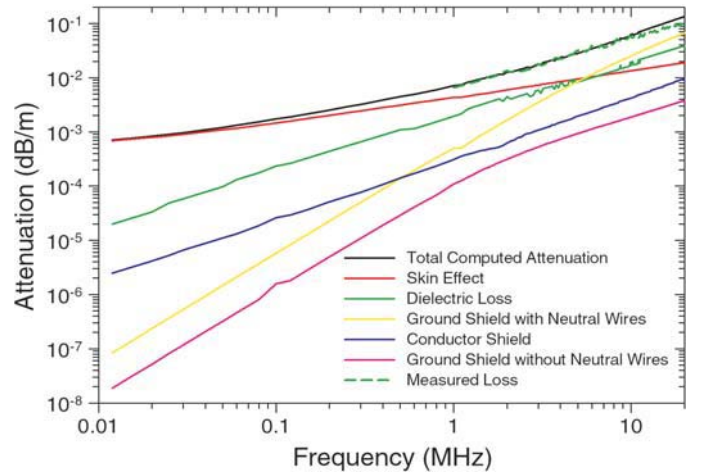


Figure 12. Loss budget for EPR2 cable. Skin effect losses dominate low frequency attenuation. At higher frequencies, the dielectric loss of this cable becomes significant, as does the effect of the ground shield loss as a result of its interaction with the neutral wires, which becomes dominant above about 4 MHz. This latter form of loss has never been analyzed in the literature but has recently been analyzed by the authors and their colleagues. Details of this loss mechanism will be published in the near future. The ground shield semicon loss without the effect of the neutral wires is shown for comparison and is much smaller. Note that at about 4 MHz three loss mechanisms make equal contributions, the sum of which add up very accurately to the measured loss of the cable.

CONCLUSIONS

The above analysis suggests that differences in cable attenuation dominate the empirical effects documented in [1], and that the difference in cable attenuation is dominated by differences in losses within the insulation, given that the structure of the cables was identical. Differences in shields, especially the ground shield, can also affect the relative high frequency attenuation of such cables. The major disappointment of this work was the inability to identify the cause of the large measured attenuation in the 3 to 7 MHz range. This attenuation does not appear to be caused by the cable and cannot be predicted based on the measured impedance characteristics of the transformer.

REFERENCES

1. Hayes, Harry L., Philip Hopkinson, Rick Piteo, and Steven Boggs. "Surge Protective Properties of Medium Voltage Underground Cable". submitted for presentation at the 2005 IEEE T&D Conference, New Orleans, LA.
2. Zhou, Li-Ming and S.A. Boggs. "Effect of High Frequency Cable Attenuation on Lightning-Induced Overvoltages on Transformers". 2002 IEEE Rural Electric Power Conference, Colorado Springs, CO, 5-7 May 2002. IEEE No. 02CH37360, ISBN 0-7803-7470-3, pp. A3-1 to A3-7.
3. Zhou, L.M. and S.A. Boggs. "Effect of Shielded Distribution Cable on Lightning-Induced Overvoltages in a Distribution System". IEEE Trans. PD-17, No. 2, April 2002. pp. 569-574.
4. Zhou, L.M. and S.A. Boggs. "Effect of Shielded Distribution Cable on Very Fast Transients". IEEE Trans PD-15, No. 3, July 2000. pp. 857-863.
5. Zhou, L.M. and S.A. Boggs. "High Frequency Attenuating Cable for Protection of Low-Voltage AC Motors Fed by PWM Inverters". Accepted for publication in IEEE Trans. PD.

BIOGRAPHIES

Joe Y. Zhou (M '04) received his Bachelor degree in electrical engineering from South China University of Technology in 1996. After graduation, he spent three years working for Siemens in the field of industrial automation. Upon completion of his Ph.D. in Materials Science at the University of Connecticut in the area of dielectric measurements of nonlinear dielectric materials, Dr. Zhou joined the Global Research Center of General Electric.

Steven Boggs (M'79, SM'92, F'93) received his Ph.D. and MBA degrees from the University of Toronto in 1972 and 1987, respectively. He spent 12 years with the Research Division of Ontario Hydro and 6 years as Director of Engineering and Research for Underground Systems, Inc. Steve is presently Director of the Electrical Insulation Research Center of the University of Connecticut and Research Professor of Materials Science, Physics, and Electrical Engineering. He is also an Adjunct Professor of Electrical Engineering at the University of Toronto. He has published widely in the areas of partial discharge measurement, high frequency phenomena in power apparatus, high field degradation of solid dielectrics, and SF₆ insulated systems. He was elected a Fellow of the IEEE for his contributions to the field of SF₆ insulated systems.